HHS Public Access

Author manuscript

Liver Int. Author manuscript; available in PMC 2017 June 01.

Published in final edited form as:

Liver Int. 2016 June ; 36(6): 874–882. doi:10.1111/liv.12933.

Induction and Contribution of β-PDGFR Signaling by Hepatic Stellate Cells to Liver Regeneration after Partial Hepatectomy in Mice

Peri Kocabayoglu[1,2], **David Y. Zhang**[1], **Kensuke Kojima**[1], **Yujin Hoshida**[1,3], and **Scott L. Friedman**[1,3]

Peri Kocabayoglu: peri.kocabayoglu@uk-essen.de; David Y. Zhang: david.y.zhang@mssm.edu; Kensuke Kojima: kentaman.k@gmail.com; Yujin Hoshida: yujin.hoshida@mssm.edu; Scott L. Friedman: scott.friedman@mssm.edu

[1]Division of Liver Diseases, Department of Medicine, Icahn School of Medicine at Mount Sinai, New York, NY, USA

[2]Department of General, Visceral and Transplant Surgery, University Hospital Essen, Germany

[3]Liver Cancer Program, Tisch Cancer Institute, Icahn School of Medicine at Mount Sinai, New York, NY

Abstract

Background—Hepatic stellate cells (HSCs) activate during injury to orchestrate the liver's inflammatory and fibrogenic responses. A critical feature of HSC activation is the rapid induction of β-PDGFR, which drives cellular fibrogenesis and proliferation; in contrast, normal liver has minimal β-PDGFR expression. While the role of β-PDGFR is well established in liver injury, its expression and contribution during liver regeneration are unknown. The aim of this study is to determine whether β-PDGFR is induced during liver regeneration following partial hepatectomy (pHx), and to define its contribution to the regenerative response.

Methods—Control mice or animals with HSC-specific β-PDGFR-depletion underwent two-thirds pHx followed by assessment of hepatocyte proliferation and expression of β-PDGFR. RNA-sequencing from whole liver tissue of both groups after pHx was used to uncover pathways regulated by β-PDGFR signaling in HSCs.

Results—β-PDGFR expression on HSCs was upregulated within 24 hours (h) following pHx in control mice, whereas absence of β-PDGFR blunted the expansion of HSCs. Mice lacking β-PDGFR displayed prolonged increases of transaminase levels within 72 h following pHx. Hepatocyte proliferation was impaired within the first 24 h based on Ki-67 and PCNA expression in β-PDGFR-deficient mice. This was associated with dysregulated growth in the β-PDGFR-deficient mice based on RNAseq with pathway analysis, and real time quantitative PCR, which demonstrated reduced expression of Hgf, Igfbp1, Mapk and Il-6.

Corresponding author: Scott L. Friedman, M.D., Icahn School of Medicine at Mount Sinai, 1425 Madison Ave., Box 1123, Room 11-70C, New York, NY 10029-6574, Tel +1 212 659 9501, Fax +1 212 849 2574, scott.friedman@mssm.edu.

Conflicts of interest

The authors have no conflicts of interest.

Conclusions—β-PDGFR is induced in HSCs following surgical pHx and its deletion in HSCs leads to prolonged liver injury. However, there is no significant difference in liver regeneration.

Keywords

receptor tyrosine kinase; liver regeneration; partial hepatectomy; pathway analysis

Introduction

Liver regeneration is a well-orchestrated yet complex response that can fully restore lost tissue mass following surgical 2/3 partial hepatectomy (pHx) of normal liver. Regeneration is remarkable in its capacity to reconstitute all the cellular elements in the new tissue without damage to the residual liver lobes. Following hepatectomy, initial signals of regeneration can be observed within 5 minutes, lasting up to 5–7 days. Events proceed sequentially through engagement of parenchymal, then non-parenchymal cell types (1). Hepatocytes first enter the cell cycle within the first 24 hours following pHx, in a wave of mitoses advancing from periportal to pericentral lobular regions (2). Next, proliferation of biliary epithelial cells and then endothelial cells begin 2–3 days after pHx, ending days ~4–5. In contrast to these resident cell types, the kinetics of hepatic stellate cell (HSC) responses, the key fibrogenic cell in liver, have not been characterized and their contribution to organ restoration is unknown.

Hepatic stellate cells (HSCs) are pericytic, vitamin-A storing cells that normally lie within the subendothelial space of Disse. In response to injury, they become activated, proliferate and migrate along the developing inflammatory septae (3).

A key and early feature of stellate cell activation is the induction of β-PDGFR, a receptor tyrosine kinase, whose expression is very low in healthy liver, but dramatically increases in HSCs during injury (4). Its expression is restricted to HSCs among resident liver cell types. The PDGF-PDGF receptor signaling network is comprised of four ligands, PDGF A-D, transducing their signals through dimeric transmembrane receptors α- and β-PDGFR, which combine as hetero- or homodimers upon ligand binding (5, 6). Ligand-induced PDGF receptor activation causes autophosphorylation of the receptor, leading to a cascade of intracellular signaling pathways that include activation of PI3-Kinase and AKT, MAPK as well as PLCγ, resulting in cell growth, chemotaxis, actin reorganization and prevention of apoptosis (7).

HSCs control the remodeling of extracellular matrix (ECM) during liver injury, not only through deposition of collagen, but also through the release of matrix-bound growth factors, including hepatocyte growth factor (HGF). ECM synthesis and remodeling are also relevant to liver regeneration, however, as ECM production is induced immediately after hepatocytes begin to proliferate following partial hepatectomy (8). In this context HSCs have been implicated as the source of remodeled ECM during liver regeneration as well (9, 10).

Recent evidence links the contribution of stromal cells, driven by β-PDGFR signaling, not only to the development of liver fibrosis, but also to inflammatory responses, regeneration and cancer (11, 12). We recently established β-PDGFR expression and signaling on HSCs as

a vital component of liver fibrosis by using mice with either HSC-specific deletion or overactivation of β-PDGFR using a Cre-Lox strategy (13). These findings established HSCs as a key source of both fibrosis and inflammatory signals following experimental liver injury. In a complementary study, the overactivation of PDGF-B ligand in transgenic mice increased the number of dysplastic lesions in the liver, and accelerated their progression towards HCC, in addition to up-regulating β-catenin expression, as well as VEGF and CD31 (14).

Sorafenib, a multi-tyrosine kinase inhibitor and currently the only medication approved for the treatment of non-resectable HCC, can delay liver regeneration following hepatic resection when administered at the time of surgery (15, 16). β-PDGFR is a target inhibited by sorafenib, yet it is uncertain whether the drug's inhibitory effect on regeneration is attributable to β-PDGFR antagonism.

In the current study we used a model of HSC-specific deletion of β-PDGFR by interbreeding β-PDGFR-floxed mice with transgenic glial fibrillary acidic protein (GFAP) -Cre mice, resulting in an HSC-specific knock down of the receptor. Combined with assessment of β-PDGFR after pHx, we have characterized the dynamics of the receptor's expression, and its functional contributions to liver homeostasis and restoration of hepatocyte mass.

Methods

Animals

In order to generate an HSC-specific deletion of β-PDGFR in the liver, β-PDGFR$^{fl/fl}$ mice (on the 129S4/SvJaeSor background), as previously described (17), were crossed with a transgenic FVB line, which expressed Cre-recombinase controlled by the glial fibrillary acidic protein (GFAP) promoter (18, 19). Transgenic GFAP-Cre mice were obtained from Jackson Laboratory (Bar Harbor, Maine). Tg(GFAP-Cre)/+;β-PDGFR$^{fl/fl}$ mice with a stellate cell-specific knock down were compared to β-PDGFR$^{fl/fl}$ mice. All animal studies were approved by the Institutional Animal Care and Use Committee at the Icahn School of Medicine at Mount Sinai and followed the National Institute of Health guidelines for animal care.

Model of Murine Liver Regeneration

Partial hepatectomy to remove 2/3 of the liver was performed on 8-week-old age-matched male mice according to a standard protocol (20). Briefly, animals were anesthetized using isoflurane (Forane, Baxter, Deerfield, IL), followed by a midline laparotomy. After division of the falciform ligament, the left lateral and median liver lobe were removed using 4-0 silk ligatures placed at the base of each lobe, followed by resection using curved microsurgery scissors. Sham operated animals received laparotomy and division of liver ligaments without ligation of the liver lobes. The peritoneum and skin were closed separately, using absorbable synthetic sutures (PDS and Monocryl, respectively, Ethicon, Bridgewater, NJ). Mice were sacrificed at indicated time points after surgery.

Liver Tests

Levels of serum aspartate aminotransferase (AST) and alanine aminotransferase (ALT) were quantified using spectrophotometry (Pointe Scientific Inc., Canton, MI).

Isolation and Culture of Primary Hepatic Stellate Cells

Hepatic stellate cells were isolated from β-PDGFR$^{fl/fl}$ GFAP-Cre negative and β-PDGFR$^{fl/fl}$ GFAP-Cre positive mice by enzymatic pronase and collagenase digestion, followed by Percoll density gradient centrifugation (21). Cells were kept in culture using Dulbecco's modified Eagle medium (DMEM) containing 10% fetal bovine serum.

Western Blot

Pieces of whole liver were homogenized using a tissue homogenizer (TissueRuptor, Qiagen, Germantown, MD), followed by centrifugation. Protein extraction from cells or whole liver was performed using lysis buffer complemented with protease inhibitor (Complete Lysis M kit, Roche Diagnostics, Indianapolis, IN) and phosphatase inhibitor (Halt Phosphatase Inhibitor Single-Use Cocktail, Thermo Scientific, Waltham, MA). Protein concentration was measured using a Bio-Rad DC kit (Bio-Rad Laboratories, Hercules, CA) and lysates were then subjected to immunoblot analysis. Blots were developed with the ECL Detection System (Amersham, Pharmacia Biotech, Buckinghamshire, England). Densitometry of bands was performed with ImageJ software (rsbweb.nih.gov/ij, NIH, Bethesda, MD). Western blot membranes were incubated with the following primary antibodies: Rabbit anti-β-PDGFR (1:500) and anti-phospho-β-PDGFR (1:500) were obtained from Santa Cruz Biotechnology, Santa Cruz, CA, rabbit anti-CD31 (1:500), rabbit anti-Ki67 (1:2500), rabbit anti-Desmin (1:1000) and rabbit anti-Calnexin (1:3,000) were from Abcam, Cambridge, England). The reactions were detected with the Fujifilm LAS-4000 system (Fujifilm Life Science, Stamford, CT), using a horseradish peroxidase-conjugated secondary antibody (Anti-rabbit IgG, Cell Signaling, Danvers, MA).

Histology and Immunohistochemical Studies

Livers were fixed in formalin, paraffin-embedded, sectioned at 4μm and routinely processed for H&E staining. Immunohistochemical staining for β-PDGFR (1:500) (Santa Cruz Biotechnology, Santa Cruz, CA), CD31 (1:500), Ki67 (1:2500) and Desmin (1:1000) (Abcam, Cambridge, England) was performed on formalin-fixed, paraffin-embedded liver sections with rabbit polyclonal antibodies. Morphometry was used to quantify stained tissue area with Bioquant image analysis software (Bioquant Image Analysis Corporation, Nashville, TN).

Reverse Transcription and Real-Time Quantitative PCR

RNA was extracted using Trizol (Life Technologies, Carlsbad, CA), followed by purification using Qiagen mini columns (Qiagen, Germantown, MD) including an on-column deoxyribonuclease treatment. One microgram of RNA was then reverse-transcribed using RNA to cDNA EcoDry Premix (double Primed) Kit (Clontech, Mountain View, CA). For quantitative real-time PCR, IQ SYBR Green Supermix (BioRad Laboratories, Hercules, CA) was used. The reaction was performed on the lightCycler480 System (Roche Diagnostics,

Indianapolis, IN). Samples were then analyzed in triplicate using Microsoft Excel software (Microsoft Corp., Redmond, WA). Data are represented as the relative expression of genes after normalizing to glyceraldehyde-3-phosphate dehydrogenase (*Gapdh*). (For a complete list of primers see Table 1.)

Expression profiling by high-throughput sequencing

Livers were removed from β-PDGFR and Δβ-PDGFR mice 72 hours following either sham operation or pHx. Each experimental condition was performed in duplicate. Whole liver mRNA was extracted as described above. The Illumina TruSeq RNA Sample Prep Kit (Illumina, Inc., San Diego, CA) was used with 2.5 μg of total RNA for the construction of sequencing libraries. RNA libraries were prepared for sequencing using standard Illumina protocols. The 100 nucleotide single end sequencing was done on an Illumina HiSeq 2000. Transcript expression levels were quantified as Fragments Per Kilobase per Megabase (FPKM) using the TopHat and Cufflinks pipeline (22).

The dataset (GSE#52234) is available at NCBI Gene Expression Omnibus database (www.ncbi.nlm.nih.gov/geo).

Bioinformatics and Statistical Analysis

Differentially modulated molecular pathways were surveyed by using Gene Set Enrichment Analysis (GSEA) (23) on a comprehensive gene set collection in the Molecular Signatures Database (MSigDB, www.broadinstitute.org/gsea/msigdb). Briefly, genes in the genome-wide transcriptome profiles were rank-ordered according to differential expression between the experimental groups to be compared based on t-statistic. Subsequently, predefined gene sets annotated with biological functions in MSigDB were mapped onto the gene list, and accumulation of each gene set on either up- or down-regulated side of the rank-ordered genes was quantitatively evaluated by using Kolmogorov–Smirnov statistic. Significance of the statistic was assessed based on null distribution of the statistic iteratively calculated by random permutation of gene IDs 1,000 times, and adjusted for multiple hypothesis testing by false discovery rate (FDR). FDR less than 0.25 was regarded as statistically significant.

Experimental results are represented as mean ± SEM and compared using Student's t-test. At least 3 independent determinations were calculated in order to generate p-values using Microsoft Excel software. A p-value < 0.05 was considered statistically significant. Statistical significance was expressed as follows: *$p<0.05$, **$p<0.001$. Prism 6 software was used to create graphs (GraphPad Software, Inc.).

Results

β-PDGFR Activation is Induced During Liver Regeneration

To first assess the induction of β-PDGFR activation during liver regeneration, we performed 2/3 pHx or sham operation on PDGFR$^{fl/fl}$ mice (controls). Whole liver lysates were analyzed via western blot at different time points following surgery (Fig. 1A). Phosphorylation of β-PDGFR could be detected as early as 24 hours after partial hepatectomy, indicating active signaling by the receptor.

We next investigated the contribution of β-PDGFR expression by HSCs during tissue regeneration. To do so, we generated a mouse line with a specific deletion of the receptor on HSCs by crossing β-PDGFR$^{fl/fl}$ mice with animals expressing Cre-recombinase under the glial fibrillary acidic protein promoter (GFAP-Cre). A thorough characterization of the model has been reported previously (13). Isolation of primary HSCs from β-PDGFR$^{fl/fl}$ GFAP-Cre positive mice (Tg(GFAP-Cre)/+;β-PDGFR$^{fl/fl}$) could confirm the knockdown of the receptor on this cell type compared to β-PDGFR$^{fl/fl}$ GFAP-Cre negative mice (Suppl. Fig. 1A). β-PDGFR$^{fl/fl}$ GFAP-Cre negative (β-PDGFR$^{fl/fl}$) and β-PDGFR$^{fl/fl}$ GFAP-Cre positive (Δβ-PDGFR) mice underwent either sham surgery or pHx. Twenty-four hours following surgery, liver sections of β-PDGFR control mice displayed expansion of β-PDGFR-positive cells, whereas β-PDGFR expression was significantly diminished in Δβ-PDGFR mice (Fig. 1B, C). Not only did this confirm the sufficient knockdown of the receptor, it also demonstrated the expansion of β-PDGFR positive cells within the liver lobule during regeneration.

Loss of β-PDGFR by HSCs increases hepatic injury during liver regeneration

To determine whether knockdown of β-PDGFR on HSCs leads to impaired regenerative capacity following partial liver resection, we performed either sham surgery or pHx in Δβ-PDGFR mice and controls. Δβ-PDGFR mice displayed early impairment of liver growth within the first 24 hours after surgery, but these differences were attenuated at later time points (Fig. 2A). However, serum alanine aminotransferase (ALT) and aspartate aminotransferase (AST) were significantly elevated in mice of Δβ-PDGFR group versus controls for up to 72 hours (Fig. 2B, C), although there were no significant differences in the extent of histologic injury (Suppl. Fig. 1B). To assess expansion of HSCs during liver regeneration, the number of desmin-positive cells were quantified in liver sections of either sham operated or mice following pHx (Suppl. Fig. 1C, D). Only in control mice were desmin-positive cells expanded after 72 hours, whereas there was no increase among animals of the Δβ-PDGFR group.

β-PDGFR expression by HSCs affects PCNA but not Ki67 in hepatocytes during liver regeneration

To assess the effect of β-PDGFR signaling by HSCs on hepatocyte proliferation during liver regeneration, we quantified Ki67 protein and proliferating cell nuclear antigen (*Pcna)* mRNA expression in hepatocytes after pHx (Fig. 3A, B). Whereas there was no difference in Ki67 between control and Δβ-PDGFR mice for up to 120 hours, whole liver *Pcna* mRNA expression was attenuated in Δβ-PDGFR animals compared to control mice following pHx (Fig. 3C).

β-PDGFR deficiency in HSCs diminishes expression of growth factors after partial hepatectomy

Since *Pcna* mRNA expression in the liver following pHx was attenuated in Δβ-PDGFR mice, we assessed the expression of key hepatocyte mitogens (Fig. 4A, B). Indeed, based on real time qPCR the mRNAs for *Hgf*, insulin-like growth factor (*Igf1)* as well as insulin-like growth factor binding protein 1 (*Igfbp1)* were markedly increased in control but not in Δβ-PDGFR mice after pHx (Fig. 4A).

We performed RNA-sequencing of whole liver mRNA from β-PDGFR$^{fl/fl}$ GFAP-Cre positive and β-PDGFR$^{fl/fl}$ GFAP-Cre negative mice. Molecular pathway analysis using gene set enrichment analysis (GSEA) revealed enrichment of several genes that were related to pathways such as the *Igf1*-pathway, as well as *Met*-, *Mapk*- and *Il6*-pathways (Fig. 4B). (For a comprehensive summary of GSEA see Supplementary Table 1).

Discussion

In the current study, we assessed the impact of β-PDGFR expression and signaling by HSCs following pHx, and its contribution to liver regeneration. Whereas Induction and enhanced signaling of the β-PDGFR during HSC activation is a hallmark of liver injury, its behavior after pHx is unknown. In liver injury models, deletion of β-PDGFR in HSCs impairs their fibrogenic potential *in vivo*, leading to decreased expression of fibrogenic markers and reduced cell proliferation. Conversely, sustained activation of the β-PDGFR receptor leads to HSC expansion in this setting (13).

No studies have previously assessed the contribution of β-PDGFR to liver regeneration. Our data indicate that β-PDGFR expression by HSCs is increased within 24 hours following pHx in a healthy liver, which is paralleled by HSC proliferation and expansion. Moreover, although histologic necrosis was similar, the increase of serum transaminase levels was more prolonged when HSCs lack β-PDGFR, which is the opposite of the impact of β-PDGFR on hepatic inflammation following liver injury, as we reported previously (13). This divergent role of β-PDGFR on hepatic inflammation between parenchymal injury and regeneration models indicates that its contribution to hepatocellular injury may be context-specific, such that the β-PDGFR signaling in HSCs promotes inflammation during injury but attenuates it following partial hepatectomy.

Mice with HSC-specific β-PDGFR knockdown displayed significantly reduced expression of key growth regulators MAPK, HGF and IGF1 and other pathways that control cellular growth. By GSEA, members of the MAPK as well as IL-6 pathway are enriched following partial hepatectomy in mice expressing the receptor, and their expression is attenuated when β-PDGFR expression by HSCs is diminished. Of these, IGFBP1 is among the most rapidly and highly induced genes within the regenerating liver. It has anti-apoptotic properties through binding and inhibition of BAK (24). The protein is up-regulated in response to IL-6 signaling following liver resection, and IGFBP1 deficiency impairs liver regeneration after pHx (25); this impairment can be rescued when a preoperative dose of IGFBP1 is administered, ultimately leading to MAPK/ERK activation and C/EBP beta expression (25).

Although there was a significant impact on growth regulatory pathways following pHx in mice lacking β-PDGFR expression on HSCs, Ki67 expression did not differ between control and Δβ-PDGFR mice, despite significant differences in *Pcna* mRNA expression. As a possible explanation, HSC activation and thus β-PDGFR expression are preceded by proliferation of other cell types and their signaling cascade, such as liver sinusoidal endothelial cells. It is also possible, that redundant signaling from other proliferative factors such as EGF and HGF compensate for the lack of β-PDGFR signaling, or even α–PDGFR signaling, should this pathway be activated in parallel. The modest effect of β-PDGFR loss

by HSCs on the proliferative response of hepatocytes may reflect inefficient Cre expression in HSCs, such that while changes in expression of growth regulatory genes are detectable, the loss of β-PDGFR following Cre-mediated recombination may not have been efficient enough to unearth an impact on hepatocyte proliferation. The GFAP-promoter used in these studies to drive Cre expression was the best available at the time; however, more recent studies have identified the lecithin-retinol acyltransferase (LRAT) (26) and β-PDGFR promoters (27) as more potent drivers of Cre-recombinase in HSCs, and their use in future studies to deplete β-PDGFR could yield a greater impact on hepatocyte proliferation. Although the GFAP promoter has been shown to be expressed in cholangiocytes, which might not make it an exclusive marker for HSCs, we have shown in our previous studies, that the sufficient deletion of a floxed allele in HSCs takes place, as confirmed on a post-transcriptional level via immunoblot (13). Several authors have used this model in order to analyze HSC physiology using GFAP-Cre (28, 29)

Also, whereas pHx was performed in uninjured liver in our studies, a more physiologic context might include the presence of liver injury. In the latter setting, β-PDGFR induction is more significant and sustained than after pHx in a normal liver, and therefore the dependence of hepatocyte proliferation on this pathway might have been more significant had injury been present. Thus, while activation of HSCs to elicit a wound healing response occurs in both settings, the continuous, iterative nature of chronic liver injury may uncover a stronger dependence of hepatocyte growth on β-PDGFR signaling by HSCs.

Our findings greatly expand and refine the observations that non-parenchymal cells support liver regeneration, as previously demonstrated in a study in which ablation of NPCs by administration of gliotoxin, since in this latter study the effect of gliotoxin is not restricted to HSCs (8). Not only did the ablation of NPCs at early time points after liver resection interfere with liver regeneration, but it delayed the termination of regeneration at later time points (8). These findings highlight a time-dependent regulatory role of NPCs in the regenerative process, but they did not define which cell types were critical to the effect, even though macrophages and sinusoidal endothelial cells both contribute significantly to liver regeneration (30, 31).

Understanding the signals underlying hepatocyte proliferation using clinically relevant models is essential to improving our ability to promote liver regeneration therapeutically. Our studies suggest that β-PDGFR signaling by HSCs provide important signals to support this response, and, moreover, that therapeutic inhibition of this pathway to attenuate fibrosis could impair hepatic regeneration, especially in the setting of chronic liver injury.

Supplementary Material

Refer to Web version on PubMed Central for supplementary material.

Acknowledgments

Financial Support

This work has been supported by grants from the Deutsche Forschungsgemeinschaft (DFG) (KO 4086/1-1 to P.K.), as well as the NIH DK056621 and NIH AA020709 (to S.L.F.), the Icahn School of Medicine Medical Scientist

Training Program NIH GM007280 (to S.L.F. and D.Y.Z.) and the NIH DK099558 and Irma T. Hirschl Trust and Dr. Harold and Golden Lamport Research Award (to Y.H.).

Mice were obtained from Dr. Philippe M. Soriano (Department of Developmental and Regenerative Biology, Icahn School of Medicine at Mount Sinai). RNA sequencing was performed by the Genomics Core, preprocessing was performed by Dr. Ke Hao and Dr. Antonio Fabio DiNarzo (Genetics and Genomic Science, Icahn School of Medicine at Mount Sinai).

Abbreviations

β-PDGFR	beta platelet-derived growth factor
HSC	hepatic stellate cell
GFAP	glial fibrillary acidic protein
bw	body weight
lw	liver weight
pHx	partial hepatectomy
ECM	extracellular matrix
AST	aspartate aminotransferase
ALT	alanine aminotransferase
HCC	hepatocellular carcinoma
mRNA	messenger ribonucleic acid
PCR	polymerase chain reaction
GAPDH	glyceraldehyde 3-phosphate dehydrogenase
H&E	hematoxylin and eosin
PCNA	proliferating cell nuclear antigen
GSEA	gene set enrichment analysis
HGF	hepatocyte growth factor
IGF1	insulin-like growth factor 1
IGFBP1	insulin-like growth factor binding protein 1
IL6	interleukin 6
NPC	non-parenchymal cell

References

1. Michalopoulos GK. Liver regeneration. J Cell Physiol. 2007; 213:286–300. [PubMed: 17559071]
2. Rabes HM. Kinetics of hepatocellular proliferation as a function of the microvascular structure and functional state of the liver. Ciba Found Symp. 1977:31–53. [PubMed: 248005]
3. Friedman SL. Hepatic stellate cells: protean, multifunctional, and enigmatic cells of the liver. Physiol Rev. 2008; 88:125–172. [PubMed: 18195085]
4. Pinzani M, Milani S, Herbst H, DeFranco R, Grappone C, Gentilini A, et al. Expression of platelet-derived growth factor and its receptors in normal human liver and during active hepatic fibrogenesis. Am J Pathol. 1996; 148:785–800. [PubMed: 8774134]

5. Seifert RA, Hart CE, Phillips PE, Forstrom JW, Ross R, Murray MJ, et al. Two different subunits associate to create isoform-specific platelet-derived growth factor receptors. J Biol Chem. 1989; 264:8771–8778. [PubMed: 2542288]
6. Wu E, Palmer N, Tian Z, Moseman AP, Galdzicki M, Wang X, et al. Comprehensive dissection of PDGF-PDGFR signaling pathways in PDGFR genetically defined cells. PLoS One. 2008; 3:e3794. [PubMed: 19030102]
7. Heldin CH, Westermark B. Mechanism of action and in vivo role of platelet-derived growth factor. Physiol Rev. 1999; 79:1283–1316. [PubMed: 10508235]
8. Nejak-Bowen KN, Orr AV, Bowen WC Jr, Michalopoulos GK. Gliotoxin-induced changes in rat liver regeneration after partial hepatectomy. Liver Int. 2013; 33:1044–1055. [PubMed: 23552057]
9. Gallai M, Sebestyen A, Nagy P, Kovalszky I, Onody T, Thorgeirsson SS. Proteoglycan gene expression in rat liver after partial hepatectomy. Biochem Biophys Res Commun. 1996; 228:690–694. [PubMed: 8941340]
10. Friedman SL. Mechanisms of hepatic fibrogenesis. Gastroenterology. 2008; 134:1655–1669. [PubMed: 18471545]
11. Kocabayoglu P, Friedman SL. Cellular basis of hepatic fibrosis and its role in inflammation and cancer. Front Biosci (Schol Ed). 2013; 5:217–230. [PubMed: 23277047]
12. Zhang DY, Friedman SL. Fibrosis-dependent mechanisms of hepatocarcinogenesis. Hepatology. 2012; 56:769–775. [PubMed: 22378017]
13. Kocabayoglu P, Lade A, Lee YA, Dragomir AC, Sun X, Fiel MI, et al. beta-PDGF Receptor Expressed by Hepatic Stellate Cells Regulates Fibrosis in Murine Liver Injury, but Not Carcinogenesis. J Hepatol. 2015
14. Maass T, Thieringer FR, Mann A, Longerich T, Schirmacher P, Strand D, et al. Liver specific overexpression of platelet-derived growth factor-B accelerates liver cancer development in chemically induced liver carcinogenesis. Int J Cancer. 2011; 128:1259–1268. [PubMed: 20506153]
15. Mollbrink A, Augsten M, Hultcrantz R, Eriksson LC, Stal P. Sorafenib prolongs liver regeneration after hepatic resection in rats. J Surg Res. 2013; 184:847–854. [PubMed: 23726434]
16. Hora C, Romanque P, Dufour JF. Effect of sorafenib on murine liver regeneration. Hepatology. 2011; 53:577–586. [PubMed: 21274878]
17. Schmahl J, Rizzolo K, Soriano P. The PDGF signaling pathway controls multiple steroid-producing lineages. Genes Dev. 2008; 22:3255–3267. [PubMed: 19056881]
18. Hernandez-Gea V, Ghiassi-Nejad Z, Rozenfeld R, Gordon R, Fiel MI, Yue Z, et al. Autophagy releases lipid that promotes fibrogenesis by activated hepatic stellate cells in mice and in human tissues. Gastroenterology. 2012; 142:938–946. [PubMed: 22240484]
19. Yang L, Jung Y, Omenetti A, Witek RP, Choi S, Vandongen HM, et al. Fate-mapping evidence that hepatic stellate cells are epithelial progenitors in adult mouse livers. Stem Cells. 2008; 26:2104–2113. [PubMed: 18511600]
20. Mitchell C, Willenbring H. A reproducible and well-tolerated method for 2/3 partial hepatectomy in mice. Nat Protoc. 2008; 3:1167–1170. [PubMed: 18600221]
21. Blomhoff R, Berg T. Isolation and cultivation of rat liver stellate cells. Methods Enzymol. 1990; 190:58–71. [PubMed: 1965004]
22. Trapnell C, Roberts A, Goff L, Pertea G, Kim D, Kelley DR, et al. Differential gene and transcript expression analysis of RNA-seq experiments with TopHat and Cufflinks. Nat Protoc. 2012; 7:562–578. [PubMed: 22383036]
23. Subramanian A, Tamayo P, Mootha VK, Mukherjee S, Ebert BL, Gillette MA, et al. Gene set enrichment analysis: a knowledge-based approach for interpreting genome-wide expression profiles. Proc Natl Acad Sci U S A. 2005; 102:15545–15550. [PubMed: 16199517]
24. Leu JI, George DL. Hepatic IGFBP1 is a prosurvival factor that binds to BAK, protects the liver from apoptosis, and antagonizes the proapoptotic actions of p53 at mitochondria. Genes Dev. 2007; 21:3095–3109. [PubMed: 18056423]
25. Leu JI, Crissey MA, Craig LE, Taub R. Impaired hepatocyte DNA synthetic response posthepatectomy in insulin-like growth factor binding protein 1-deficient mice with defects in C/EBP beta and mitogen-activated protein kinase/extracellular signal-regulated kinase regulation. Mol Cell Biol. 2003; 23:1251–1259. [PubMed: 12556485]

26. Mederacke I, Hsu CC, Troeger JS, Huebener P, Mu X, Dapito DH, et al. Fate tracing reveals hepatic stellate cells as dominant contributors to liver fibrosis independent of its aetiology. Nat Commun. 2013; 4:2823. [PubMed: 24264436]

27. Henderson NC, Arnold TD, Katamura Y, Giacomini MM, Rodriguez JD, McCarty JH, et al. Targeting of alphav integrin identifies a core molecular pathway that regulates fibrosis in several organs. Nat Med. 2013; 19:1617–1624. [PubMed: 24216753]

28. Kisseleva T, Cong M, Paik Y, Scholten D, Jiang C, Benner C, et al. Myofibroblasts revert to an inactive phenotype during regression of liver fibrosis. Proc Natl Acad Sci U S A. 2012; 109:9448–9453. [PubMed: 22566629]

29. Michelotti GA, Xie G, Swiderska M, Choi SS, Karaca G, Kruger L, et al. Smoothened is a master regulator of adult liver repair. J Clin Invest. 2013; 123:2380–2394. [PubMed: 23563311]

30. Forbes SJ, Rosenthal N. Preparing the ground for tissue regeneration: from mechanism to therapy. Nat Med. 2014; 20:857–869. [PubMed: 25100531]

31. Ding BS, Cao Z, Lis R, Nolan DJ, Guo P, Simons M, et al. Divergent angiocrine signals from vascular niche balance liver regeneration and fibrosis. Nature. 2014; 505:97–102. [PubMed: 24256728]

Key points

1. We show that β-PDGFR is induced on HSCs following partial hepatectomy.
2. We characterize the dynamics of β-PDGFR expression on HSCs, and its functional contributions to liver homeostasis and restoration of hepatocyte mass.
3. Using a HSC-specific knock-down model of β-PDGFR in mice, we demonstrate that β-PDGFR deficiency on HSCs leads to prolonged hepatic injury following pHx.
4. Using RNA sequencing β-PDGFR deficiency in HSCs diminishes expression of growth factors after partial hepatectomy.

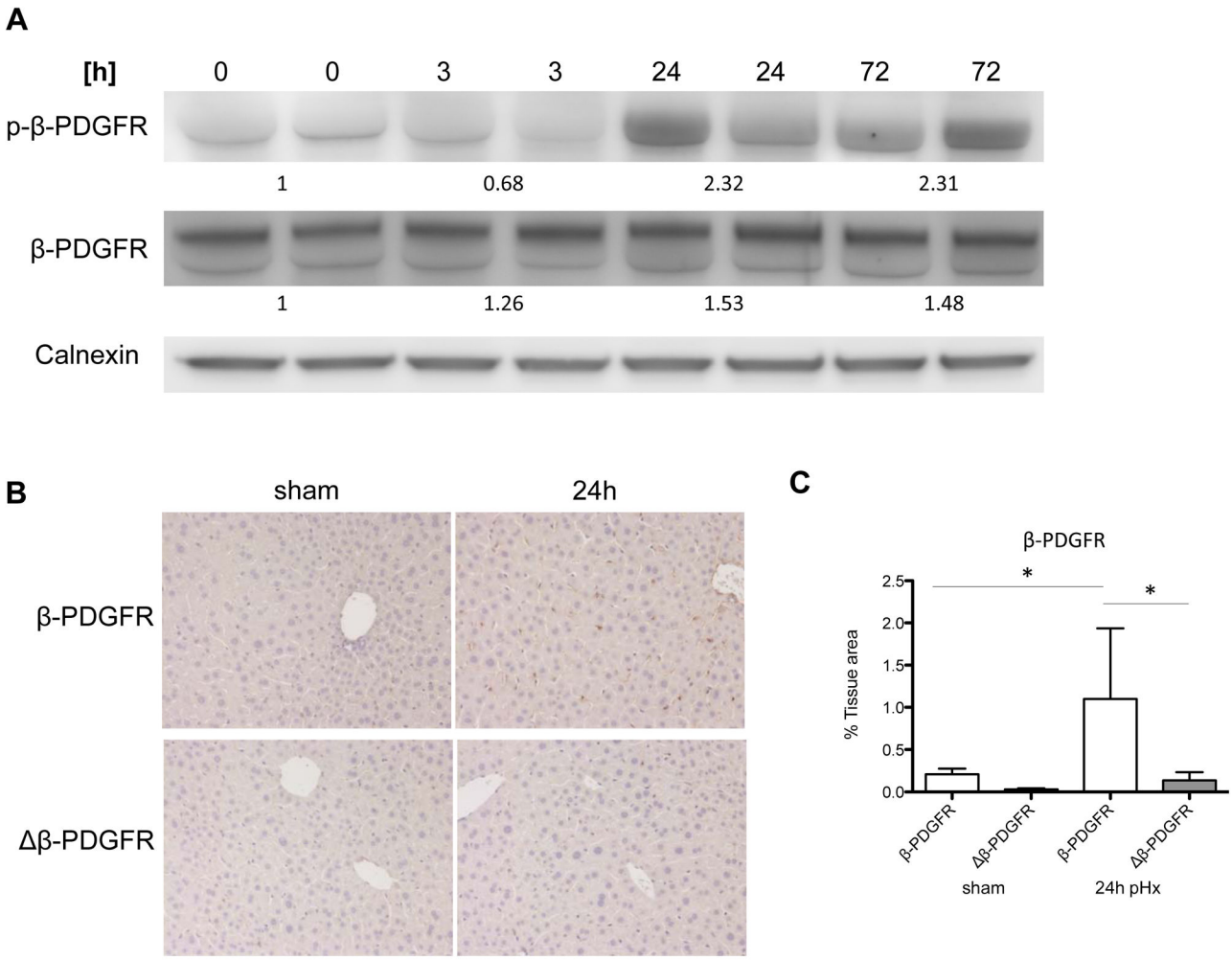

Fig. 1. Activation of β-PDGFR occurs after partial Hepatectomy

(A) Mice underwent partial hepatectomy, after which livers were collected at indicated time points. Western blot of whole liver lysates demonstrating increased expression of β-PDGFR and its phosphorylation as early as 24 hours following surgery. Average value of densitometric analysis relative to control (0h) normalized to Calnexin is shown underneath bands.

(B) β-PDGFR staining of paraffin embedded liver sections of β-PDGFR and control mice depicts a significant increase of β-PDGFR expression following partial hepatectomy, and confirmed lack thereof in Δβ-PDGFR mice (magnification 200x).

(C) Graph shows percentage of tissue area positive for β-PDGFR measured by morphometry in β-PDGFR and Δβ-PDGFR mice 24 hours following either sham operation of partial hepatectomy.

Data represent the mean value of n=5 per group (∗$p<0.05$, error bars indicate SEM). [h], hour following partial hepatectomy, pHx, partial hepatectomy.

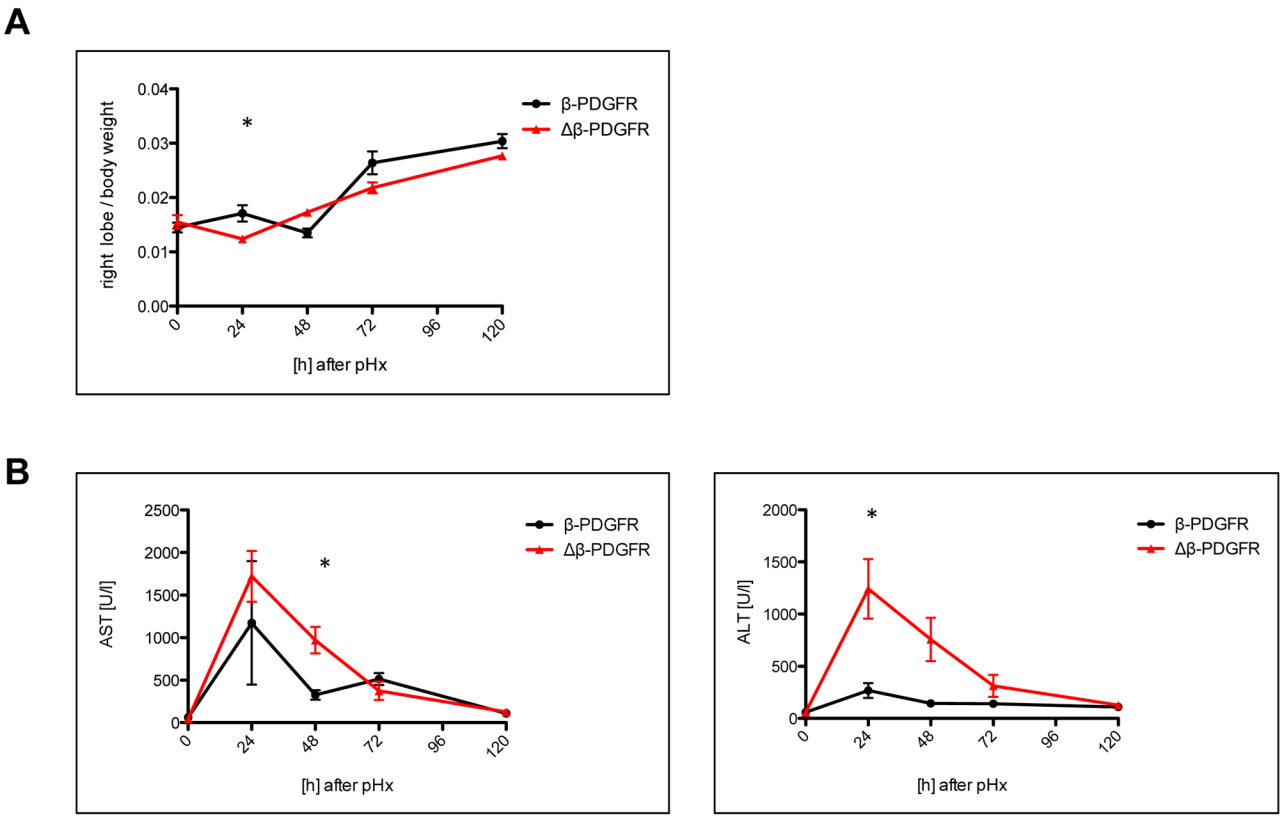

Fig. 2. Δβ-PDGFR mice exhibit increased levels of transaminases following partial liver resection

(A) Graph shows residual liver weight to body weight ratio at indicated time points following partial hepatectomy in each experimental group. Liver weight of Δβ-PDGFR showed a significant lack of weight gain when compared to control mice at 24hours following partial hepatectomy, but there was almost equal development after 48hours in both groups.

(B) Levels of serum AST and ALT during the course of liver regeneration following surgery. Δβ-PDGFR responded to liver resection with a higher increase of serum transaminases between 24 and 48 hours when compared to β-PDGFR mice. Levels of transaminases showed a parallel course in both groups after 72hours.

All figures represent the mean of at least n=5 animals per experimental group. (*$p<0.05$, error bars indicate SEM). PHx, partial hepatectomy.

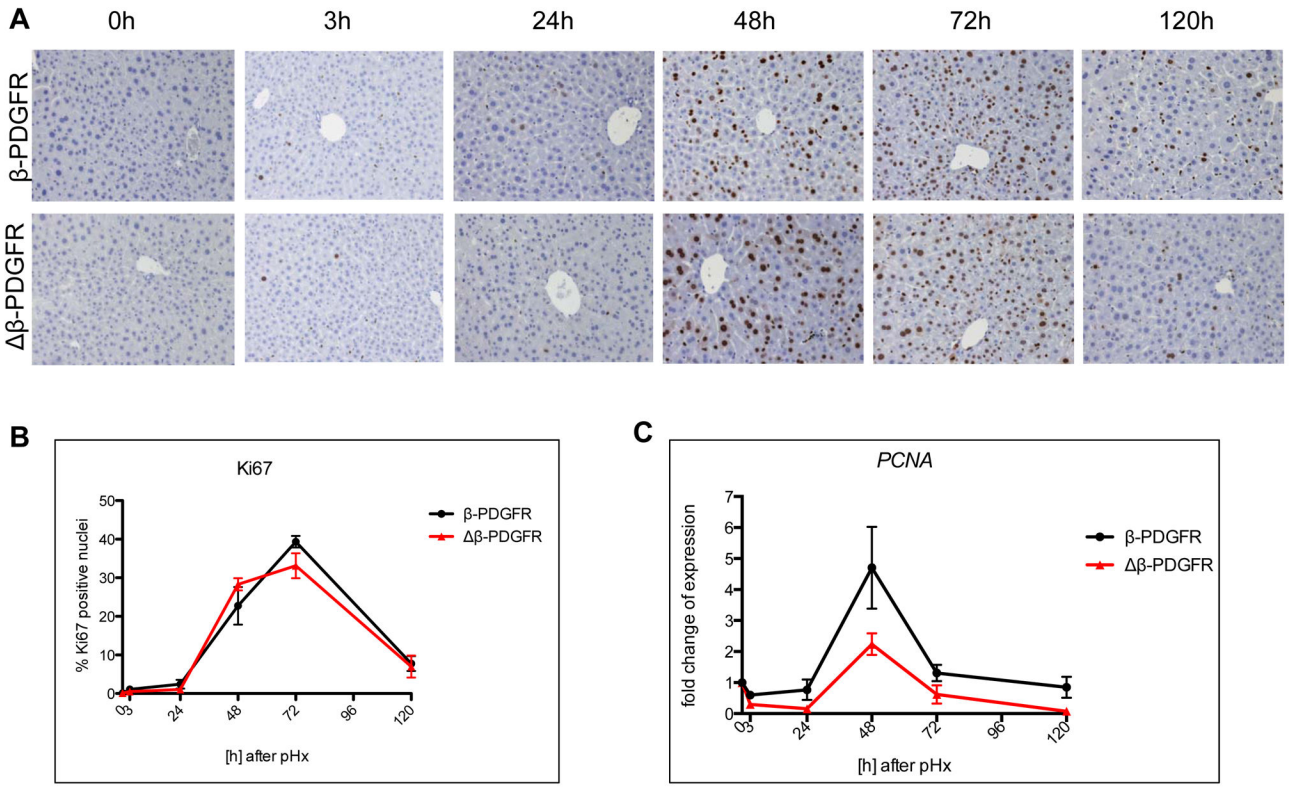

Fig. 3. Knock down of β-PDGFR on HSCs does not lead to decreased levels of hepatocyte proliferation upon partial hepatectomy

(A) Ki67 staining of paraffin embedded liver sections of β-PDGFR and control mice shows equal proliferation of hepatocytes in Δβ-PDGFR and control mice at the indicated timepoints after surgery (magnification 200x).

(B) Graph shows quantification of Ki67 positive hepatocytes in relation to all hepatocytes per field.

(C) Whole liver mRNA expression of *Pcna* after partial hepatectomy shows decreased, but not significantly reduced levels within the Δβ-PDGFR group versus control animals.

All figures represent the mean of at least n=5 animals per experimental group. mRNA is normalized to *Gapdh.* (Error bars indicate SEM). PHx, partial hepatectomy.

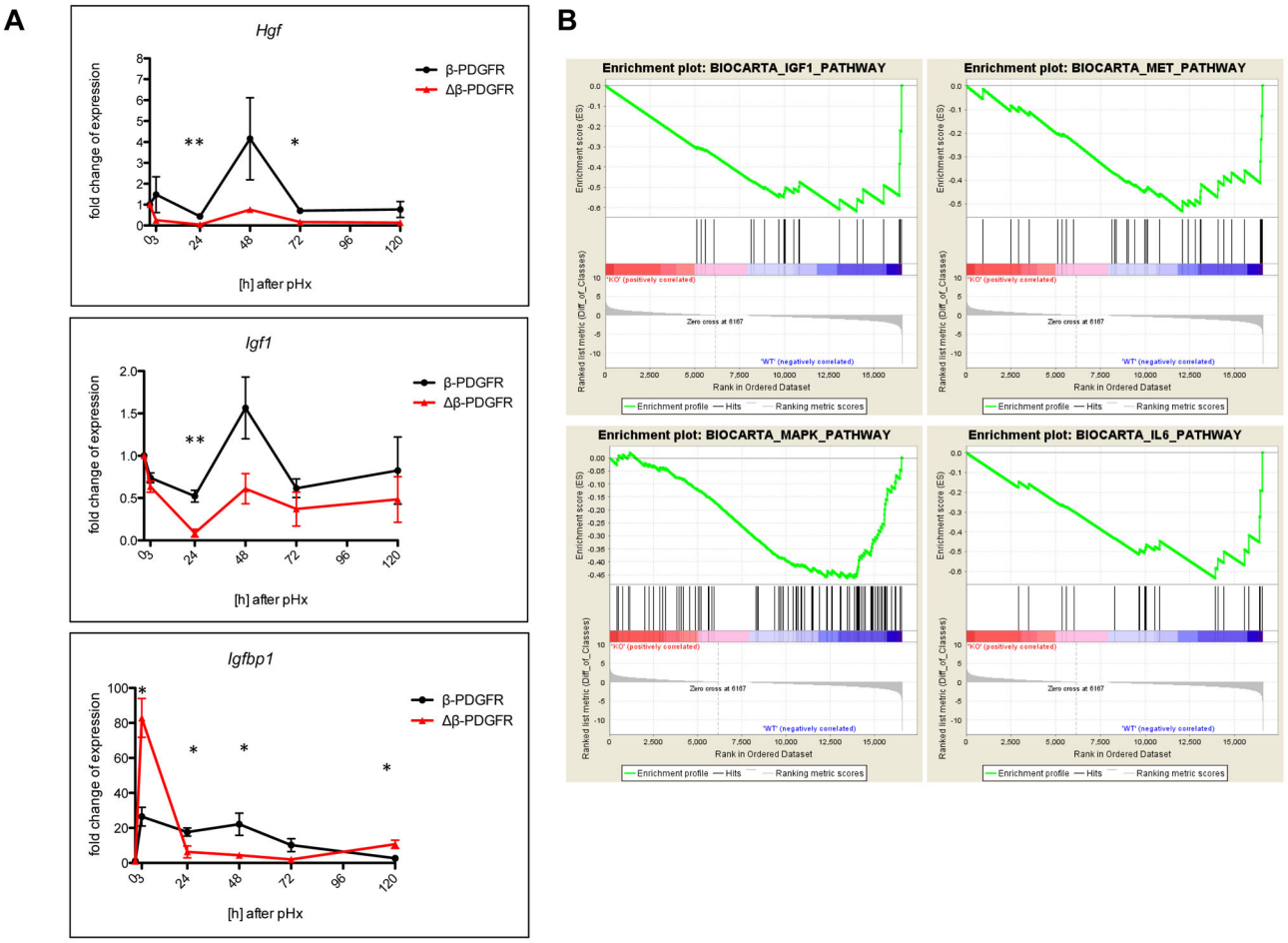

Fig. 4. Knock down of β-PDGFR on HSCs leads to reduced expression of growth factors confirmed by expression profiling via RNA sequencing

(A) Whole liver mRNA expression of *Hgf*, *Igf1* and *Igfbp1* at indicated timepoints following partial heaptectomy shows decreased levels of growth factors in the Δβ-PDGFR group compared with β-PDGFR. Levels differ especially within the first 48 hours and show an equal course thereafter. All timepoints represent the mean of at least n=5 animals per experimental group. mRNA is expressed normalized to *Gapdh* (*p<0.05, **p<0.01, error bars indicate SEM).

(B) Down-regulated molecular pathways in liver tissues from Δβ-PDGFR mice 72 hours after sham hepatectomy identified by Gene Set Enrichment Analysis (GSEA). Genes in the genome-wide transcriptome profiles were rank-ordered in horizontal axis (left: up-regulated in Δβ-PDGFR mice, right: up-regulated in wild type mice), and each pathway gene set was mapped onto the rank-ordered gene list (black bars indicate member genes in each gene set). Accumulation of each gene set on either Δβ-PDGFR or wild type side was quantitatively measured by using Kolmogorov–Smirnov statistic, i.e., top or bottom peak of the green line projected to y-axis as enrichment score. Significance of the gene set modulation was assessed by false discovery rate (FDR). (See Methods for the details.) PHx, partial hepatectomy.

Table 1

List of Primers

Name	Sequence
mouse *β-Pdgfr* F	5′-ACTACATCTCCAAAGGCAGCACCT-3′
mouse *β-Pdgfr* R	5′-TGTAGAACTGGTCGTTCATGGGCA-3′
mouse *Gapdh* F	5′-CAATGACCCCTTCATTGACC-3′
mouse *Gapdh* R	5′-GATCTCGCTCCTGGAAGATG-3′
mouse *Pcna* F	5′-TGCTCTGAGGTACCTGAACT-3′
mouse *Pcna* R	5′-TGCTTCCTCATCTTCAATCT-3′
mouse *Igf1* F	5′-GAATGTTCCCCCAGCTGTTTC-3′
mouse *Igf1* R	5′-CATTGCGCAGGCTCTATCTG-3′
mouse *Igfbp1* F	5′-AGATCGCCGACCTCAAGAAATGGA-3′
mouse *Igfbp1* R	5′-TGTTGGGCTGCAGCTAATCTCTCT-3′
mouse *Hgf* F	5′-TTCATGTCGCCATCCCCTATG-3′
mouse *Hgf* R	5′-CCCCTGTTCCTGATACACCT-3′